



# Fabrication of partially biobased carbon fibers from novel lignosulfonate–acrylonitrile copolymers

Qin Ouyang<sup>1,\*</sup>, Keqiang Xia<sup>1,2</sup>, Dapeng Liu<sup>1,3</sup>, Xuefeng Jiang<sup>1,2</sup>, Hongbo Ma<sup>1</sup>, and Yousi Chen<sup>1</sup>

<sup>1</sup>National Engineering Laboratory for Carbon Fiber Preparation Technology, Ningbo Institute of Material Technology and Engineering, Chinese Academy of Sciences, Ningbo 315201, China

<sup>2</sup>College of Material Science and Chemical Engineering, Ningbo University, Ningbo 315211, China

<sup>3</sup>Nano Science and Technology Institute, University of Science and Technology of China, Suzhou 215123, China

Received: 8 December 2016

Accepted: 4 March 2017

Published online:

10 March 2017

© Springer Science+Business Media New York 2017

## ABSTRACT

Lignin, as an abundant carbon-rich renewable resource, is a promising precursor for carbon fibers. However, due to the poor spinnability of lignin, a great challenge comes from the spinning of precursor fibers. In this work, a series of lignosulfonate–acrylonitrile (LS–AN) copolymers with different LS contents were prepared by a two-step process consisting of esterification and free radical copolymerization. In this strategy, lignin was used as a macromer and chemically bonded to acrylonitrile segment, resulting in significant improvement of the spinnability. Continuous long precursor fibers with a dense structure were successfully prepared from these copolymers by a wet spinning technique and then converted into carbon fibers by thermal stabilization and carbonization. The LS–AN copolymers were characterized by FTIR, GPC, and rheological method. The results confirmed the macromolecular characteristic of the LS–AN copolymers. A hanging lantern model was proposed to describe the molecular structure of the LS–AN copolymers. Effect of the LS–AN copolymers on the microstructure and mechanical properties of carbon fibers was investigated by SEM, single fiber tensile testing, XRD, and HRTEM. The results demonstrated the feasibility of developing partially biobased carbon fibers from the novel LS–AN copolymers.

## Introduction

Carbon fibers are versatile materials for a broad range of applications. They are known as the most important reinforcements for advanced composites. Carbon fiber-reinforced composites exhibit not only exceptional properties, such as lightweight, high strength,

high stiffness, fatigue resistance, and corrosion resistance, but also excellent designability, processability, and application flexibility, and therefore have been widely used in aerospace, general aviation, and sporting goods [1]. Most noteworthy, a rapid increase in demand for carbon fibers emerges in a variety of industrial applications during the recent

Address correspondence to E-mail: o\_yang@126.com; ouyangqin@nimte.ac.cn

decade [2]. In particular, in the automotive industry and construction industry, the foreseeable demand for carbon fibers is very huge [3–5]. However, currently, the limited availability and the high cost of carbon fibers have seriously restricted their widespread application in the industrial fields [5]. This is mainly due to that more than 90% of the commercial carbon fibers are prepared from petroleum-derived polyacrylonitrile (PAN) which is expensive and not sustainable [2]. In order to solve this problem, alternative raw materials for carbon fibers must be identified and implemented [6].

Renewable biopolymers or polymers from biogenic resources, such as cellulose and lignin, are very attractive sources for carbon fibers [6]. As for lignin, it is especially meaningful to be converted into carbon fibers. Lignin is the second most abundant biopolymer, only after cellulose, on earth [7]. However, in contrast to cellulose, lignin has not yet been converted into value-added products on a large scale so far [6, 8, 9]. Most of lignin has been directly burned as fuel for energy recovery, which causes grievous waste of the natural resources [10]. Because of the abundant availability and the carbon-rich phenolic chemical structure, lignin is regarded as a very promising precursor for carbon fibers [8]. Lignin has a carbon content as high as above 60% and plenty of aromatic structure units, which theoretically satisfies the basic requirements for carbon fibers.

Lignin has been studied as a precursor for preparation of carbon fibers for more than 50 years, and a great deal of research has focused on the development of lignin-based carbon fibers in recent years [11]. However, substantial progress is still not achieved up to now. All reported lignin-derived carbon fibers have significantly lower mechanical properties as compared with the commercial PAN-based carbon fibers and thus are not suitable for practical application [12, 13]. There are many challenges in the process to prepare carbon fibers from lignin. Among them, a great one comes from the spinning of precursor fibers [14]. Lignin is a complex amorphous polymer with a cross-linked network structure and a lower and widely distributed molecular weight, instead of the linear long chains such as PAN. In addition, lignin has a large number of active hydroxyl groups and various impurities [6, 15, 16]. All these factors make lignin difficult to spin into continuous and strong fibers.

Many researches have dealt with the improvement the spinnability of lignin [16–19]. Baker et al. [16] reported that hardwood lignin was purified with organic solvents to eliminate impurities for enhancing its melt spinnability, and carbon fibers with tensile strength of 0.51 GPa and tensile modulus of 28.6 GPa were obtained. However, the melt-spun pure lignin fibers must be stabilized at an extremely low heating rate of 0.01 °C/min; otherwise, the fibers cannot maintain their form. Chatterjee et al. [20, 21] used different acid anhydrides to react with lignin and found that the esterified lignins were highly compatible with melt-extrusion processing for preparation of fibers. The esterification reaction consumed the reactive hydroxyl groups of lignin which avoided the intermolecular cross-linking reaction taking place during melt spinning [21]. However, the esterified lignin fibers could be difficult to be stabilized due to that the unreactive ester groups would not cross-link during stabilization. For this reason, Zhang and Ogale [22] used a partially esterified lignin and a dry spinning technique to prepare fibers which were successfully processed into carbon fibers with tensile modulus of 52 GPa and tensile strength of up to 1.0 GPa.

The most widely used approach is to blend lignin with other linear spinnable polymers, since continuous long fibers can be easily obtained. Up to now, a series of common polymers including poly(vinyl alcohol) (PVA) [23, 24], poly(ethylene oxide) (PEO) [18, 25–28], poly(ethylene terephthalate) (PET) [19, 29], polypropylene (PP) [19, 30], poly(lactic acid) (PLA) [14, 31], and PAN [2, 32–37] have been used to blend with lignin to prepare precursor fibers and convert into carbon fibers. Among which, PAN seems to be more suitable to blend with lignin for preparation of carbon fibers, since it is the same usable precursor for carbon fibers and will not decompose into volatile fragments during thermal stabilization and carbonization [14, 31]. Zoltek and Weyerhaeuser have developed a novel low-cost carbon fiber from lignin/PAN blend using a solution-based wet spinning technique. As reported by them in 2014, the tensile strength and tensile modulus of the lignin/PAN blend-based carbon fibers have reached up to 2.24 and 217 GPa, respectively [33].

Recently, lignin/PAN blend has been investigated by different research teams for preparation of carbon fibers [2, 32–37]. However, because lignin only acted as a heterogeneous filler in the blend, some lignin

was dissolved out during wet spinning process, creating production problems [33]. Furthermore, some macrovoids were formed in the fibers, which may result in the decline of mechanical properties of carbon fibers. In order to inhibit the loss of lignin and avoid the formation of macrovoids, we have prepared a novel lignosulfonate–acrylonitrile (LS–AN) copolymer, via a two-step process consisting of esterification and free radical copolymerization, and proved it is a suitable precursor for preparation of carbon fibers [38]. In this strategy, lignin was used as a macromer and chemically bonded to acrylonitrile segment. Thus, the difficult problems, namely the loss of lignin and the formation of macrovoids, during wet spinning were well solved. In the present work, we have prepared a series of LS–AN copolymers with different LS contents. Continuous long precursor fibers have been prepared from these copolymers by a wet spinning technique and then converted into carbon fibers by thermal stabilization and carbonization. The carbon fibers were characterized by scanning electron microscopy (SEM), single fiber tensile testing, X-ray diffraction (XRD), and high-resolution transmission electron microscopy (HRTEM) for insight of the effect of the novel LS–AN copolymer precursors on the microstructure and mechanical properties of carbon fibers.

## Experimental

### Materials

A commercial lignin product, calcium lignosulfonate (LS) with the purity of 96%, was purchased from Aladdin Industrial Corporation and used after being purified by desalting using dilute sulfuric acid. Acryloyl chloride (AC) and triethylamine (TEA) were analytically pure and also purchased from Aladdin Industrial Corporation and used as received. Analytically pure dimethyl sulfoxide (DMSO) was obtained from Sinopharm Chemical Reagent Co. Ltd. and used as received. Industrial-grade acrylonitrile (AN) was purchased from Sinopec Shanghai Petrochemical Co. Ltd. and treated by vacuum distillation before use to remove the inhibitor. Chemically pure  $\alpha,\alpha$ -azoisobutyronitrile (AIBN) was purchased from Shanghai No.4 Reagent & H.v Chemical Co. Ltd. and used as an initiator after crystallization in ethanol.

### Preparation

A series of LS–AN copolymers with different LS contents were prepared by a two-step process consisting of esterification and free radical copolymerization. First, esterified LS was synthesized. Fifty grams of purified LS was dissolved in 200 g of DMSO at 60 °C under stirring. The solution was then cooled in an ice bath, and 30 g of AC was slowly added into the above solution at 0 °C in 1 h, and then, the mixture was to react at 30 °C for 22 h. After the reaction was complete, the resulting product was precipitated in diethyl ether, centrifuged, and washed with ethanol several times. The esterified LS was obtained after drying at 60 °C under vacuum for 24 h. Second, LS–AN copolymers were prepared by copolymerization of the esterified LS with AN at a total concentration of 25 wt% in DMSO solvent. The mass ratio of LS to AN in feed varied from 10:90, 15:85, 20:80, and 25:75 to 30:70. The required amounts of LS and AN were mixed into 90 g of DMSO in a three neck round-bottom flask equipped with a mechanical stirrer, which was preheated to 60 °C under nitrogen atmosphere. About 5 wt% of AIBN, based on LS, was added as initiator and the copolymerization reaction was carried out under nitrogen atmosphere at 60 °C for 22 h. All the dopes were added into deionized water, and the LS–AN copolymers were obtained by filtration, washing, and drying at 60 °C under vacuum for 24 h.

The LS–AN copolymer-based precursor fibers were by a wet spinning technique. The spinning solution was prepared by dissolving 20 g of the LS–AN copolymer in 46.6 g of DMSO at 60 °C, which was deaerated by stewing at 50 °C. The spinning solution was then extruded through a spinneret (50 holes, 0.1 mm diameter) under 0.3 MPa nitrogen into a DMSO/H<sub>2</sub>O (60:40 w/w, 60 °C) mixture used as coagulation bath. The speed of the first rollers for collecting the nascent fibers was 5 m/min. The nascent fibers were washed and stretched synchronously in two water baths of 70 and 80 °C. The total stretch ratios were 2.4. The stretched fibers were then finished by going through an oil agent bath, which was an oil-in-water emulsion, for isolation and protection. Subsequently, the fibers were dried on hot rollers of 110 and 120 °C in sequence. During this process, water was removed, and the microvoids in the fibers collapsed, resulting in a dense structure. Finally, the

precursor fibers were spooled onto a winding machine (Kamitsu Co., Ltd).

The LS–AN copolymer-based precursor fibers were converted into carbon fibers by thermal stabilization followed by carbonization. For thermal stabilization, the precursor fibers were placed in an air furnace heated from room temperature to 250 °C with a heating rate of 10 °C/min and maintained at 250 °C for 1 h. Then the thermo-stabilized fibers were carbonized at 1400 °C for 10 min with a heating rate of 10 °C/min under nitrogen atmosphere (GSL-1700X high-temperature furnace, MTI Corporation).

The prepared samples, including LS–AN copolymers and their solutions, precursor fibers and carbon fibers, were coded as LS–AN 10, LS–AN 15, LS–AN 20, LS–AN 25, and LS–AN 30, in turn.

## Characterization

Transmission FTIR spectra of the LS–AN copolymers were recorded on a Thermo Nicolet Nexus 470 FTIR spectrometer using a thin film technique in 4000–400  $\text{cm}^{-1}$  range. Thirty-two scans were acquired at a resolution of 4  $\text{cm}^{-1}$ . Thin films of the LS–AN copolymers were prepared by using a solution casting method as reported in Ref. [38]. The relative content of LS in the LS–AN copolymers was determined by calculating the ratio of the two characteristic absorption peaks at 1510 and 2243  $\text{cm}^{-1}$ . The details of this method were described in Ref. [38].

The average molecular weight and molecular weight distribution of the LS–AN copolymers were determined by gel permeation chromatography (GPC) (TOSOH HLC-8320GPC) using a refractive index detector. The samples were dissolved in 0.01 mol/L LiBr/DMF solution at a concentration of 1 mg/mL and filtered using 0.45- $\mu\text{m}$  PTFE syringe filter prior to analysis. The instrument was calibrated with a set of polystyrene standards purchased from TOSOH CORPORATION.

The viscosity and stress of the LS–AN copolymer solutions were measured as a function of shear rate by a HAAKE MARS III rheometer (Thermo Fisher, USA) in a conical cylinder geometry (cup diameter: 27 mm, bob diameter: 25 mm). All the LS–AN copolymer solutions were prepared at concentration of 24 wt% in DMSO solvent and measured at a same temperature of 60 °C.

The micromorphology of the LS–AN copolymer-based precursor fibers and carbon fibers was

examined using a Hitachi S-4800 field emission scanning electron microscope (SEM). All the samples were sputter-coated with gold before imaging.

Tensile strength of the individual carbon fibers was measured according to the BS ISO 11566:1996 standard with a Donghua University XQ-1/XD-1 single fiber tester. The gauge length and crosshead speed were 25 mm and 5 mm/min, respectively. Fiber diameters were determined using an indicating micrometer. Data were reported as the average of 20 fibers per sample, and the standard deviation was also calculated.

XRD patterns of the carbon fibers were obtained from a Bruker X-ray diffractometer (D8, Advance) using nickel-filtered Cu  $K_{\alpha}$  radiation ( $\lambda = 0.154$  nm). The interlayer spacing ( $d_{002}$ ) and the crystallize size ( $L_c$ ,  $L_a$ ) were calculated by using the Bragg's formula and Scherrer equation, respectively.

The microstructure of the LS–AN copolymer-based carbon fibers was examined by a FEI Tecnai F20 high-resolution transmission electron microscope (HRTEM) using a bright-field imaging mode. The carbon fibers were first grinded with ethanol in an agate mortar, and then placed in glass sample bottle and dispersed using ultrasonic wave. The ultrathin films of the carbon fibers were taken out by copper microgrids coated with amorphous carbon thin films. After the ethanol was evaporated, the samples were then analyzed by HRTEM.

## Results and discussion

### Characterization of LS–AN copolymers

Figure 1 shows the FTIR spectra of the LS–AN copolymers. A sharp peak at 2243  $\text{cm}^{-1}$  is assigned to  $\text{C}\equiv\text{N}$  stretching vibration in AN unit [39]. A peak at about 1721  $\text{cm}^{-1}$  is corresponding to the stretching vibration of  $\text{C}=\text{O}$  group which is incorporated by the esterification reaction of LS with AC [38]. The peaks at 1426, 1510, and 1600  $\text{cm}^{-1}$  are attributed to the aromatic ring of LS unit [3]. As shown in Fig. 1, from LS–AN 10 to LS–AN 30, the 1721 and 1510  $\text{cm}^{-1}$  peaks continue to increase. In the meantime, the 2243  $\text{cm}^{-1}$  peak gradually decreases in intensity. According to the Lambert–Beer's law,  $A = \varepsilon bc$ , where  $A$  is the absorbance,  $\varepsilon$  is the molar absorption coefficient,  $b$  is the thickness of sample (cm), and  $c$  is the mole concentration (mol/cm), the relative content of

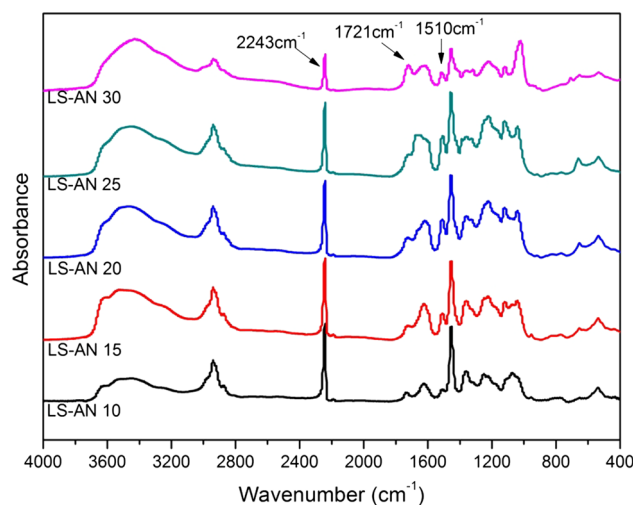


**Figure 1** FTIR spectra of LS-AN copolymers.

LS in the LS-AN copolymers can be determined by calculating the ratio of the two characteristic absorption peaks at 1510 and 2243  $\text{cm}^{-1}$ . The details of this method were described in Ref. [38]. The results are listed in Table 1. With the increase in LS content in feed, the relative content of LS in the LS-AN copolymers increases accordingly. It indicates that LS as a macromer has been successfully copolymerized with AN. On the other hand, a broad and strong peak at about 3500  $\text{cm}^{-1}$ , corresponding to the O-H stretching of hydroxyl groups in LS, still exists. It means only partial hydroxyl groups of LS have been converted into esters. However, these survived hydroxyl groups can take place cross-linking reaction with each other during stabilization, which is very necessary for the formation of stabilized structure.

The molecular weight and its distribution of the LS-AN copolymers were determined by GPC. The GPC curves of the LS-AN copolymers are presented in Fig. 2. As can be seen from Fig. 2, from LS-AN 10 to LS-AN 30, the GPC curves gradually shift to the

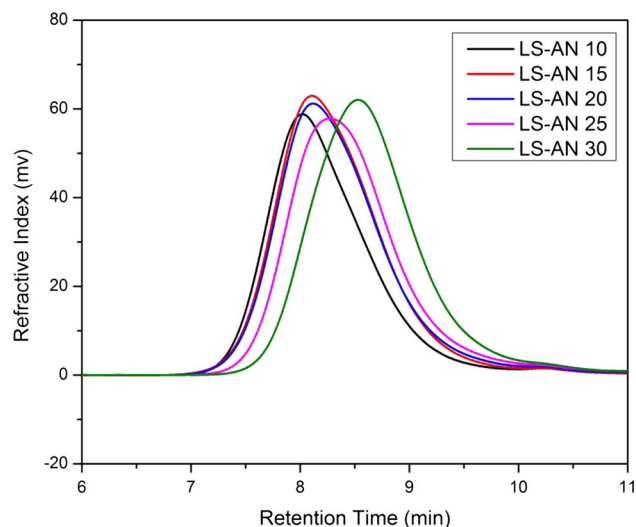


**Figure 2** GPC curves of LS-AN copolymers.

direction of higher retention time, indicating a decrease trend in the molecular weight. As shown in Table 1, both the number average molecular weight ( $M_n$ ) and weight average molecular weight ( $M_w$ ) of the LS-AN copolymers continue to decrease with the increase in LS content in feed. This is mainly because, in order to obtain a relatively high conversion, the initiator has been increased with the increase of LS in feed. In addition, the bulky structure and some unesterified hydroxyl groups of LS may also play an important role in hindering the free radical copolymerization reaction. The residue of some unesterified hydroxyl groups in the LS molecules, acting as radical scavenger, may result in the inhibition effect on the free radical copolymerization reaction [40].

The viscosity and stress of the LS-AN copolymer solutions were measured as a function of shear rate, shown in Fig. 3a, b, respectively. Both the viscosity and stress of the LS-AN copolymer solutions decrease with the increase in LS content, which is

**Table 1** LS content and molecular weight of LS-AN copolymers

Code	LS content		Molecular weight and its distribution		
	In feed (wt%)	In copolymer (wt%)	$M_n$ ( $10^4$ g/mol)	$M_w$ ( $10^4$ g/mol)	PDI ( $M_w/M_n$ )
LS-AN 10	10	11.8	4.27	17.80	4.17
LS-AN 15	15	18.3	3.50	15.31	4.38
LS-AN 20	20	24.6	3.09	14.66	4.72
LS-AN 25	25	30.2	2.47	11.88	4.81
LS-AN 30	30	38.1	1.77	8.73	4.94

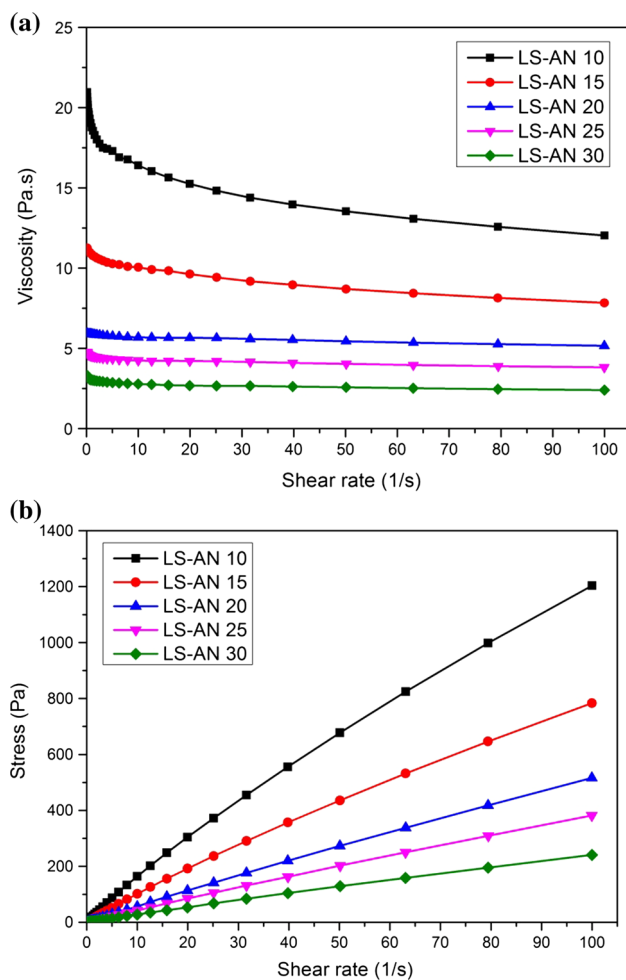


**Figure 3** **a** Viscosity and **b** stress as a function of shear rate of LS-AN copolymer solutions.

related to the decrease in molecular weight of LS-AN copolymers as shown in Table 1. With the decrease in molecular weight of the LS-AN copolymers, the viscosity of the solutions decreases significantly. In addition, typical shear-thinning behavior of non-Newtonian fluid can be observed in Fig. 3a. In particular, LS-AN 10 and LS-AN 15 have a more pronounced shear-thinning behavior below  $10 \text{ s}^{-1}$ , where a significant decrease in viscosity with the increase in shear rate. The shear-thinning behavior, as a typical characteristic of polymer solution, is mainly related to the disentanglement and orientation of macromolecular chains in solution [41]. In a polymer solution, macromolecular chains are entangled due to the intermolecular interactions. However, under high shear stress, the intermolecular interactions may be destroyed, and some of the entangled macromolecular chains will become oriented along

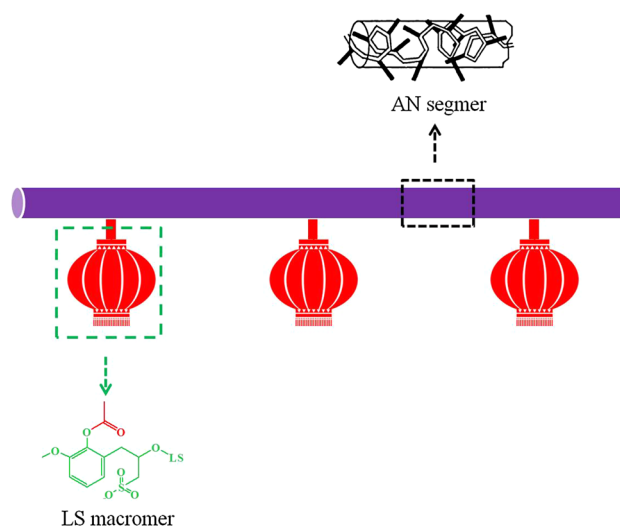


**Figure 4** Schematic of the macromolecular structure of LS-AN copolymer.

the shear direction [34]. As a result, the resistance to motion of the macromolecular chains is reduced and the viscosity of the solution is decreased. This phenomenon has further confirmed the macromolecular characteristic of the LS-AN copolymers.

As reported in the literature, LS is in the form of spherical particles [15]. This spherical conformation makes LS difficult to spin into fibers. PAN is in the form of linear long chains. Due to the intramolecular repulsion of adjacent nitrile groups, PAN chain has a rigid and irregular helical conformation [42]. This rod-like conformation endues PAN with excellent spinnability. Here, LS has been used as a macromer and chemically bonded to the AN segment. Figure 4 shows a schematic of the macromolecular structure of the LS-AN copolymer. LS molecules, such as little lanterns, have been hanged one by one along the rod of AN segment. The LS-AN copolymer, as a whole, endues the hanging LS molecules with the linear conformation and good spinnability.

### Morphology of precursor fibers

Figure 5 shows photograph of the precursor fibers prepared from the LS-AN copolymers by a wet spinning technique. During the spinning process, all the LS-AN copolymers exhibited excellent spinnability. Continuous long precursor fibers have been collected by a winding machine. All the LS-AN copolymers-based precursor fibers have good plasticity and tenacity. SEM was used to characterize the

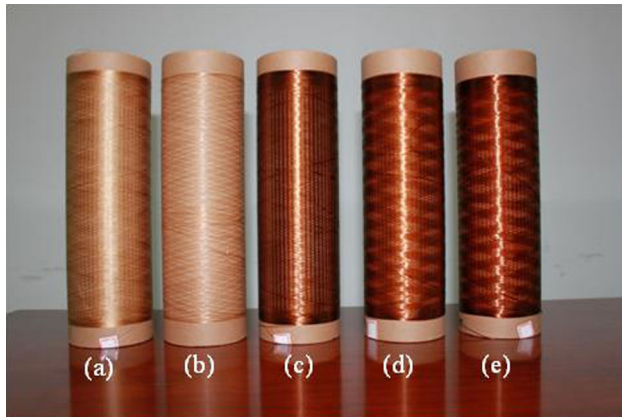


**Figure 5** Photograph of the LS–AN copolymer-based precursor fibers. *a* LS–AN 10, *b* LS–AN 15, *c* LS–AN 20, *d* LS–AN 25, *e* LS–AN 30.

micromorphology of the precursor fibers. Figure 6 shows SEM images of surface and cross section of the precursor fibers. All the precursor fibers show a dense structure without any visible macrovoid defects. The difficult problems of the loss of lignin and the formation of macrovoids during the wet spinning of the lignin/PAN blend system have been well solved. In addition, all the precursor fibers show a round and homogeneous cross section. It is probably due to that the hydrophilicity of the LS–AN copolymers has been improved significantly by introducing hydrophilic LS macromer into the copolymers [15]. The enhanced hydrophilicity makes the rates of counter diffusion and phase separation during coagulation decrease, which is conducive to formation of a round and homogeneous cross section [43].

### Morphology of carbon fibers

Carbon fibers prepared from the LS–AN copolymer-based precursor fibers by thermal stabilization and carbonization were also characterized by SEM. Figure 7 shows the SEM images of the LS–AN copolymer-based carbon fibers. As inherited the micromorphology from the precursor fibers, all the carbon fibers also show a dense structure without any visible macrovoid defects. As reported in the literature, the macrovoid defects are hardly avoided during wet spinning as for the blend system of lignin/PAN due to the loss of lignin and/or phase separation [5]. Carbon fibers are known as brittle materials, and their mechanical properties are highly dependent on the number and size of the defects [44, 45]. Thus,

the absence of the macrovoid defects will help to enhance the mechanical properties of carbon fibers.

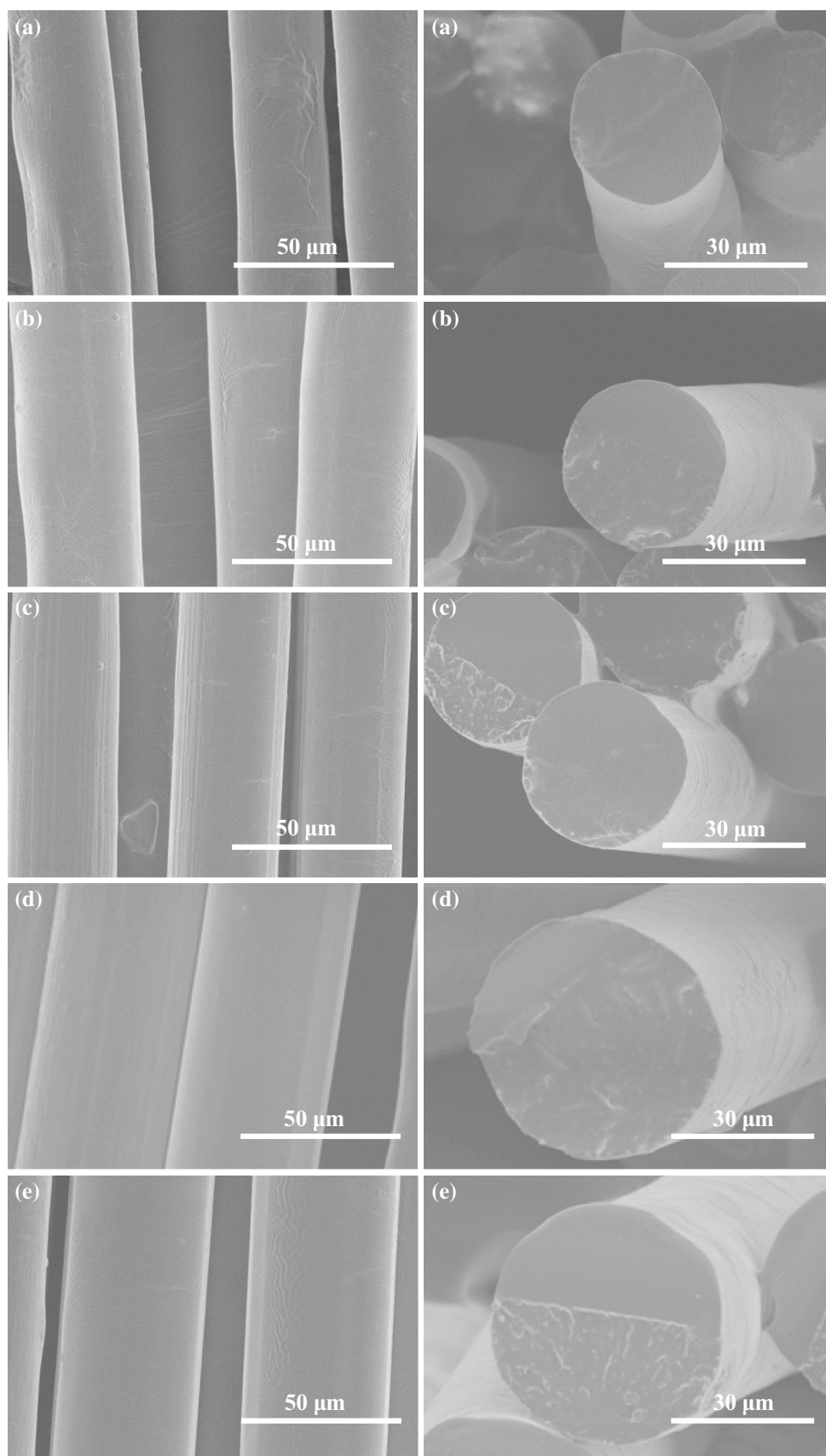
### Mechanical properties of carbon fibers

Figure 8 shows the tensile strength and fiber diameter of all the LS–AN copolymer-based carbon fibers. The carbon fibers of LS–AN 10, LS–AN 15, and LS–AN 20 have an average tensile strength of about  $649 \pm 52$ ,  $623 \pm 45$ , and  $645 \pm 58$  MPa, respectively. Considering the testing error, the difference in tensile strength of these three kinds of carbon fibers is quite small. It indicates that introducing a certain amount of LS as a macromer into the precursor would not exert adverse effect on the mechanical properties of final carbon fibers. However, to further increase the content of LS, the tensile strength of carbon fibers begins to decrease. The carbon fibers of LS–AN 25 and LS–AN 30 display an average tensile strength of about  $496 \pm 50$  and  $468 \pm 60$  MPa, respectively. As compared to the carbon fibers of LS–AN 10, the tensile strength of the carbon fibers of LS–AN 25 and LS–AN 30 decreases to some extent.

A significant increase in fiber diameter from LS–AN 10 to LS–AN 30 is shown in Fig. 8. The carbon fibers of LS–AN 10 have an average fiber diameter of about  $19.2 \mu\text{m}$ , while the carbon fibers of LS–AN 20 have an average fiber diameter of about  $24.9 \mu\text{m}$ . The latter has increased by about 30% as compared to the former. The fiber diameter of the carbon fibers of LS–AN 30 has further increased to about  $32.1 \mu\text{m}$ , which is about 1.7 times of the carbon fibers of LS–AN 10. The significant increase in fiber diameter is mainly attributed to the decrease in molecular weight of the LS–AN copolymers. Because all the spinning solutions have a same polymer concentration, the LS–AN copolymer with a lower molecular weight results in a lower viscosity spinning solution. Thus, under the same spinning conditions, namely the same spinning pressure and stretching speed, the LS–AN copolymer with a lower molecular weight can be extruded out of the spinneret at a faster rate because of the lower viscosity. A faster extrusion rate has decreased the actual drawing ratio, resulting in a larger fiber diameter.

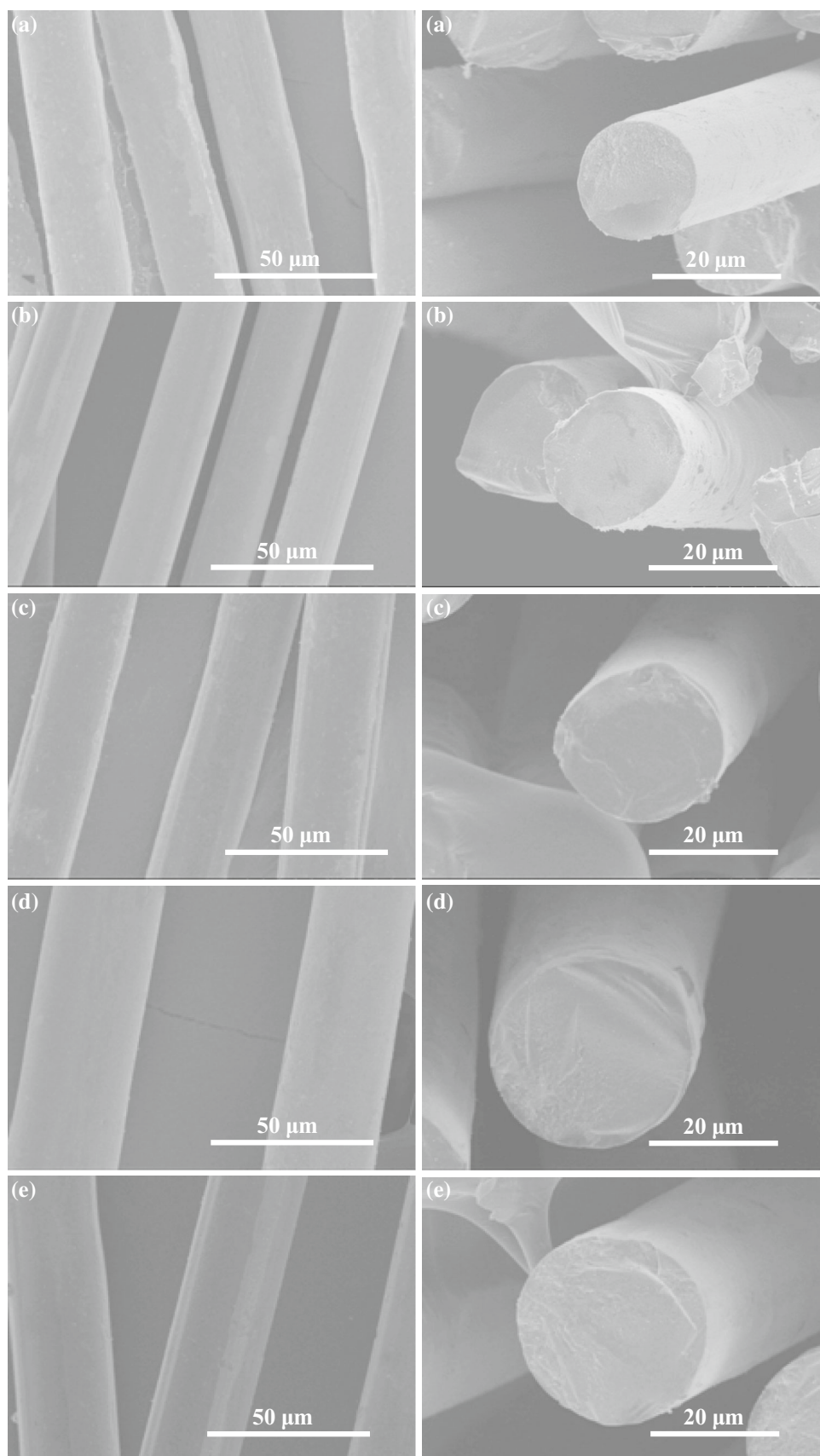
Previous studies have shown that the tensile strength of carbon fiber is constantly decreased with the increase in fiber diameter [18, 46]. In the present work, because all the carbon fibers have a large diameter, the tensile strength is still too low to be

**Figure 6** SEM images of the LS-AN copolymer-based precursor fibers. **a** LS-AN 10, **b** LS-AN 15, **c** LS-AN 20, **d** LS-AN 25, **e** LS-AN 30.





**Figure 7** SEM images of the LS–AN copolymer-based carbon fibers. **a** LS–AN 10, **b** LS–AN 15, **c** LS–AN 20, **d** LS–AN 25, **e** LS–AN 30.



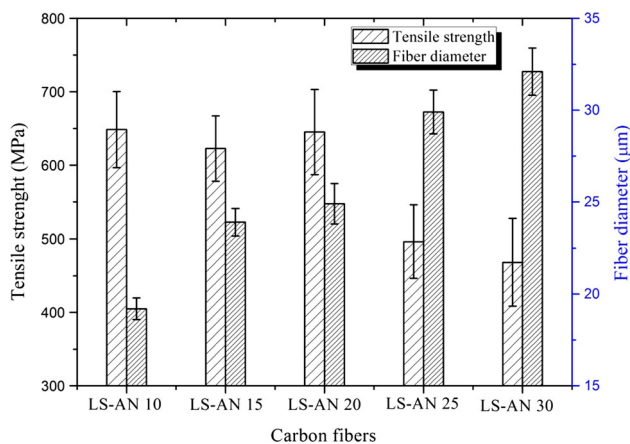


**Figure 8** Tensile strength and fiber diameter of the LS-AN copolymer-based carbon fibers.

satisfied for practical applications. However, the mechanical properties of the LS-AN copolymer-based carbon fibers are expected to be enhanced by a further decrease in diameter and a simultaneous increase in orientation of the precursor fibers under stretching, which are necessary for preparation of high-performance carbon fibers [42].

### Structural characterization of carbon fibers

Figure 9 shows the XRD patterns of the LS-AN copolymer-based carbon fibers. The curves are shifted vertically with respect to each other in order to show details of the peaks for all samples. As can be seen from Fig. 9, all the patterns exhibit one strong and broad peak corresponding to the 002 diffraction. In addition, the 10 and 11 diffraction peaks are also observed, but they are very weak. Thus, it can be inferred that the LS-AN copolymer-based carbon fibers only have a turbostratic structure. The 002 reflection is attributed to the stacking of carbon hexagonal net layers, which is the basic structural unit in carbon materials and generally called “crystallites,” even though the basal planes are stacked in parallel without regularity [47]. From LS-AN 10 to LS-AN 30, this peak shifts slightly to the low-angle side and become narrower. It means that the introduced LS unit exerts a certain affect on the stacking of carbon hexagonal net layers. The interlayer spacing,  $d_{002}$ , was obtained from the 002 reflection peak by using Bragg’s formula.

$$d_{002} = \frac{\lambda}{2 \sin \vartheta} \quad (1)$$

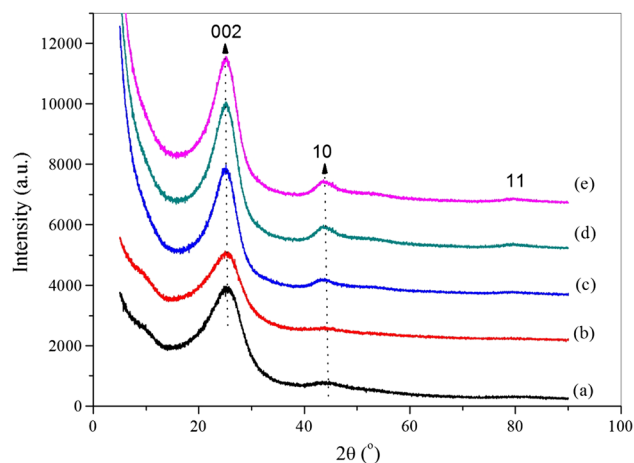


**Figure 9** XRD patterns of the LS-AN copolymer-based carbon fibers. *a* LS-AN 10, *b* LS-AN 15, *c* LS-AN 20, *d* LS-AN 25, *e* LS-AN 30.

The results are listed in Table 2. All the LS-AN copolymer-based carbon fibers show a much larger value of  $d_{002}$  ( $>0.35$  nm) as compared to the normal value, 0.3354 nm, for graphite. It has confirmed a similar turbostratic structure of these carbon fibers. However, a significant change rule in  $d_{002}$  is observed. From LS-AN 10 to LS-AN 30,  $d_{002}$  has gradually increased from 0.3500 to 0.3534 nm. It should be attributed to the amorphous carbon derived from the LS units, which has hindered the carbon hexagonal net layers from closely stacking.

The crystallite size along the  $c$ -axis,  $L_c$ , was also obtained from the 002 reflection peak by using the Scherrer equation. In the Scherrer equation, the shape factor  $K$  is assume to be 0.9 [48], and  $\beta$  is the full width at half maximum intensity (FWHM). The results are summarized in Table 2.

$$L_c = \frac{K\lambda}{\beta \cos \vartheta} \quad (2)$$

All the LS-AN copolymer-based carbon fibers have a small value of  $L_c$  ( $<1.5$  nm). It means that the parallel stacks are only of two or three layers [47]. Interestingly, the  $L_c$  shows a continuous increase from 1.1 nm of LS-AN 10 to 1.4 nm of LS-AN 25. It means introducing more LS unit into the precursor is conducive to increasing the crystallite size.

The crystallite size along the  $a$ -axis,  $L_a$ , was calculated from the 11 diffraction peak by using the Scherrer equation. A constant value of 1.84 is employed for the shape factor  $K$  in the Scherrer equation [48].

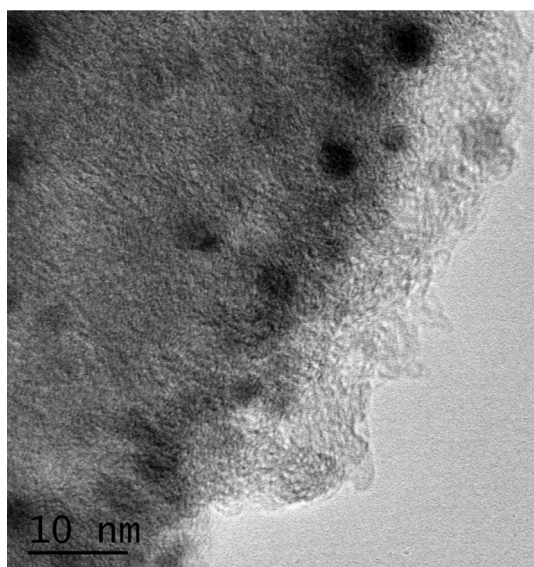
**Table 2** XRD parameters of the LS–AN copolymer-based carbon fibers

Sample	(002)				(10)		
	$2\theta$ (°)	$d_{002}$ (nm)	FWHM (°)	$L_c$ (nm)	$2\theta$ (°)	FWHM (°)	$L_a$ (nm)
LS–AN 10	25.43	0.3500	7.41	1.10	44.24	5.52	3.18
LS–AN 15	25.39	0.3506	7.28	1.12	44.14	5.15	3.40
LS–AN 20	25.34	0.3512	5.89	1.38	43.90	4.74	3.69
LS–AN 25	25.27	0.3522	5.83	1.40	43.96	4.44	3.94
LS–AN 30	25.18	0.3534	5.86	1.39	43.97	4.09	4.28

$$L_a = \frac{K\lambda}{\beta \cos \vartheta} \quad (3)$$

The  $L_a$  shows a similar change trend as the  $L_c$ , namely, from LS–AN 10 to LS–AN 30,  $L_a$  increases gradually. It has confirmed that introducing more LS unit into the precursor is conducive to increasing the crystallite size. A gradual increase in  $L_c$  and  $L_a$  would be attributed to that LS contains numerous aromatic units. These structural units can be involved in the construction of carbon hexagonal net layers and thus promote the formation and growth of the crystallite. Though the crystallite size increases significantly with the increase in the amount of LS unit in the precursor, the LS–AN copolymer-based carbon fibers still keep a turbostratic structure.

HRTEM was used to further confirm the turbostratic structure of the LS–AN copolymer-based carbon fibers. Figure 10 shows a typical HRTEM image with magnification of 250,000 times of the carbon fiber LS–AN 30. As can be seen from Fig. 10, the typical lattice structure of graphite is not found,

**Figure 10** HRTEM image of the carbon fiber LS–AN 30.

but only the turbostratic structure can be observed. Interestingly, a lot of spheres are distributed in the amorphous carbon. The sizes of the spheres range from about 5–10 nm, which are probably derived from the LS units. As mentioned above, LS is considered as in the form of spherical particles [15]. Thus, the HRTEM results have confirmed the hanging lantern structure model of the LS–AN copolymer as proposed in Fig. 4. These carbon nanospheres may endow the LS–AN copolymer-based carbon fibers with some special properties and potential applications, which will be studied in the future.

## Conclusions

In the present work, a series of lignosulfonate–acrylonitrile (LS–AN) copolymers with different LS contents were prepared by a two-step process consisting of esterification and free radical copolymerization. In this strategy, lignin was used as a macromer and chemically bonded to acrylonitrile segment, which endowed the spherical LS with the linear macromolecular conformation and good spinnability. Continuous long precursor fibers were successfully prepared from these copolymers by a wet spinning technique and then converted into carbon fibers by thermal stabilization and carbonization. All the precursor fibers and carbon fibers showed a dense structure without any visible macrovoid defects. The difficult problems of the loss of lignin and the formation of macrovoids during the wet spinning of the lignin/PAN blend system were well solved. Introducing a certain amount of LS as a macromer into the precursor would not exert adverse effect on the mechanical properties of final carbon fibers. Though the crystallite size increases significantly with the increase in the amount of LS unit in the precursor, the LS–AN copolymer-based carbon fibers still keep a turbostratic structure, where carbon nanospheres derived from the spherical LS units were included.

## Acknowledgements

Financial support by the National Natural Science Foundation of China (No. 21404111) is gratefully acknowledged.

## References

- [1] Morgan P (2005) Carbon fibers and their composites. CRC Press, New York
- [2] Ding R, Wu HC, Thunga M, Bowler N, Kessler MR (2016) Processing and characterization of low-cost electrospun carbon fibers from organosolv lignin/polyacrylonitrile blends. *Carbon* 100:126–136
- [3] Mainka H, Täger O, Körner E, Hilfert L, Busse S, Edelmann FT, Herrmann AS (2015) Lignin—an alternative precursor for sustainable and cost-effective automotive carbon fiber. *J Mater Res Technol* 4(3):283–296
- [4] Mainka H, Hilfert L, Busse S, Edelmann F, Haak E, Herrmann AS (2015) Characterization of the major reactions during conversion of lignin to carbon fiber. *J Mater Res Technol* 4(4):377–391
- [5] Baker DA, Rials TG (2013) Recent advances in low-cost carbon fiber manufacture from lignin. *J Appl Polym Sci* 130(2):713–728
- [6] Frank E, Steudle LM, Ingildeev D, Sporl JM, Buchmeiser MR (2014) Carbon fibers: precursor systems, processing, structure, and properties. *Angew Chem Int Edit* 53(21):5262–5298
- [7] Sen S, Patil S, Argyropoulos DS (2015) Thermal properties of lignin in copolymers, blends, and composites: a review. *Green Chem* 17(11):4862–4887
- [8] Schreiber M, Vivekanandhan S, Cooke P, Mohanty AK, Misra M (2014) Electrospun green fibres from lignin and chitosan: a novel polycomplexation process for the production of lignin-based fibres. *J Mater Sci* 49:7949–7958. doi:10.1007/s10853-014-8481-z
- [9] Laurichesse S, Averous L (2014) Chemical modification of lignins: towards biobased polymers. *Prog Polym Sci* 39(7):1266–1290
- [10] Ragauskas AJ, Beckham GT, Bidy MJ, Chandra R, Chen F, Davis MF, Davison BH, Dixon RA, Gilna P, Keller M, Langan P, Naskar AK, Saddler JN, Tschaplinski TJ, Tuskan GA, Wyman CE (2014) Lignin valorization: improving lignin processing in the biorefinery. *Science* 344:1246813. doi:10.1126/science.1246843
- [11] Chatterjee S, Saito T (2015) Lignin-derived advanced carbon materials. *Chemsuschem* 8(23):3941–3958
- [12] Souto F, Calado V, Pereira N (2015) Carbon fiber from lignin: a literature review. *Materia-Rio De Janeiro* 20(1):100–114
- [13] Ogale AA, Zhang M, Jin J (2016) Recent advances in carbon fibers derived from biobased precursors. *J Appl Polym Sci* 133(45):1–13. doi:10.1002/APP.43794
- [14] Thunga M, Chen K, Grewell D, Kessler MR (2014) Bio-renewable precursor fibers from lignin/poly(lactide) blends for conversion to carbon fibers. *Carbon* 68:159–166
- [15] Hatakeyama H, Hatakeyama T (2009) Lignin structure, properties, and applications. *Biopolymers*. Springer, Berlin
- [16] Baker DA, Gallego NC, Baker FS (2012) On the characterization and spinning of an organic-purified lignin toward the manufacture of low-cost carbon fiber. *J Appl Polym Sci* 124(1):227–234
- [17] Sudo K, Shimizu K, Nakashima N, Yokoyama A (1993) A new modification method of exploded lignin for the preparation of a carbon fiber precursor. *J Appl Polym Sci* 48(8):1485–1491
- [18] Kadla JF, Kubo S, Venditti RA, Gilbert RD, Compere AL, Griffith W (2002) Lignin-based carbon fibers for composite fiber applications. *Carbon* 40(15):2913–2920
- [19] Kubo S, Kadla JF (2005) Lignin-based carbon fibers: effect of synthetic polymer blending on fiber properties. *J Polym Environ* 13(2):97–105
- [20] Chatterjee S, Clingenpeel A, McKenna A, Rios O, Johs A (2014) Synthesis and characterization of lignin-based carbon materials with tunable microstructure. *Rsc Adv* 4(9):4743–4753
- [21] Chatterjee S, Jones EB, Clingenpeel AC, McKenna AM, Rios O, McNutt NW, Keffer DJ, Johs A (2014) Conversion of lignin precursors to carbon fibers with nanoscale graphitic domains. *ACS Sustain Chem Eng* 2(8):2002–2010
- [22] Zhang M, Ogale AA (2014) Carbon fibers from dry-spinning of acetylated softwood kraft lignin. *Carbon* 69:626–629
- [23] Otani S, Fukuoka Y, Igarashi B, Sasaki K (1969) Method for producing carbonized lignin fiber. US patent 3461082
- [24] Ago M, Okajima K, Jakes JE, Park S, Rojas OJ (2012) Lignin-based electrospun nanofibers reinforced with cellulose nanocrystals. *Biomacromolecules* 13(3):918–926
- [25] Kubo S, Kadla JF (2004) Poly(ethylene oxide)/organosolv lignin blends: relationship between thermal properties, chemical structure, and blend behavior. *Macromolecules* 37(18):6904–6911
- [26] Brodin I, Ernstsson M, Gellerstedt G, Sjöholm E (2012) Oxidative stabilisation of kraft lignin for carbon fibre production. *Holzforschung* 66(2):141–147
- [27] Imel AE, Naskar AK, Dadmun MD (2016) Understanding the impact of poly(ethylene oxide) on the assembly of lignin

- in solution toward improved carbon fiber production. *ACS Appl Mater Interfaces* 8(5):3200–3207
- [28] Dallmeyer I, Lin LT, Li YJ, Ko F, Kadla JF (2014) Preparation and characterization of interconnected, kraft lignin-based carbon fibrous materials by electrospinning. *Macromol Mater Eng* 299(5):540–551
- [29] Svinterikos E, Zuburtikudis I (2016) Carbon nanofibers from renewable bioresources (lignin) and a recycled commodity polymer poly(ethylene terephthalate). *J Appl Polym Sci* 133(37):1–12. doi:10.1002/APP.43936
- [30] Kubo S, Yoshida T, Kadla JF (2007) Surface porosity of lignin/PP blend carbon fibers. *J Wood Chem Technol* 27(3–4):257–271
- [31] Wang SC, Li Y, Xiang HX, Zhou Z, Chang TK, Zhu MF (2015) Low cost carbon fibers from bio-renewable lignin/poly(lactic acid) (PLA) blends. *Compos Sci Technol* 119:20–25
- [32] Liu HC, Chien AT, Newcomb BA, Davijani AAB, Kumar S (2016) Stabilization kinetics of gel spun polyacrylonitrile/lignin blend fiber. *Carbon* 101:382–389
- [33] Husman G (2014) Development and commercialization of a novel low-cost carbon fiber. Presentation at 2014DOE Hydrogen and Fuel Cells Program and Vehicle Technologies Program Annual Merit Review and Peer Evaluation Meeting, Oak Ridge National Laboratory
- [34] Oroumei A, Fox B, Naebe M (2015) Thermal and rheological characteristics of biobased carbon fiber precursor derived from low molecular weight organosolv lignin. *ACS Sustain Chem Eng* 3(4):758–769
- [35] Liu HC, Chien AT, Newcomb BA, Liu YD, Kumar S (2015) Processing, structure, and properties of lignin- and CNT-incorporated polyacrylonitrile-based carbon fibers. *ACS Sustain Chem Eng* 3(9):1943–1954
- [36] Dong XZ, Lu CX, Zhou PC, Zhang SC, Wang LY, Li DH (2015) Polyacrylonitrile/lignin sulfonate blend fiber for low-cost carbon fiber. *Rsc Adv* 5(53):42259–42265
- [37] Seydibeyoglu MO (2012) A novel partially biobased PAN-lignin blend as a potential carbon fiber precursor. *J Biomed Biotechnol* 2012:1–8. doi:10.1155/2012/598324
- [38] Xia KQ, Ouyang Q, Chen YS, Wang XF, Qian X, Wang L (2016) Preparation and characterization of lignosulfonate-acrylonitrile copolymer as a novel carbon fiber precursor. *ACS Sustain Chem Eng* 4(1):159–168
- [39] Ouyang Q, Wang XH, Wang XL, Huang J, Huang XW, Chen YS (2016) Simultaneous DSC/TG analysis on the thermal behavior of PAN polymers prepared by aqueous free-radical polymerization. *Polym Degrad Stab* 130:320–327
- [40] Maradur SP, Kim CH, Kim SY, Kim BH, Kim WC, Yang KS (2012) Preparation of carbon fibers from a lignin copolymer with polyacrylonitrile. *Synth Met* 162(5–6):453–459
- [41] Cifre JGH, La Torre JGD (2004) Orientation of polymer chains in dilute solution under shear: effect of chain model and excluded volume. *Macromol Theor Simul* 13(3):273–279
- [42] Ouyang Q, Chen Y, Wang X, Ma H, Li D, Yang J (2015) Supramolecular structure of highly oriented wet-spun polyacrylonitrile fibers used in the preparation of high-performance carbon fibers. *J Polym Res* 22(12):1–10
- [43] Ren FZ, Lu CX, Liang XY, Wu GP, He F, Ling LC (2004) Influence of amination on the structure of a PAN nascent filament during wet spinning. *New Carbon Mater* 19(4):268–274
- [44] Wang H, Xiao H, Lu Y, Jiang J (2016) The catalytic effect of boron nitride on the mechanical properties of polyacrylonitrile-based carbon fiber. *J Mater Sci* 51:10690–10700. doi:10.1007/s10853-016-0079-1
- [45] Chae HG, Newcomb BA, Gulgunje PV, Liu Y, Gupta KK, Kamath MG, Lyons KM, Ghoshal S, Pramanik C, Giannuzzi L (2015) High strength and high modulus carbon fibers. *Carbon* 93:81–87
- [46] Kubo S, Uraki Y, Sano Y (1998) Preparation of carbon fibers from softwood lignin by atmospheric acetic acid pulping. *Carbon* 36(7–8):1119–1124
- [47] Iwashita N (2016) Chapter 2—X-ray powder diffraction, materials science and engineering of carbon. Tsinghua University Press, Beijing
- [48] Cuesta A, Dhamelincourt P, Laureyns J, Martinez-Alonso A, Tascon JMD (1998) Comparative performance of X-ray diffraction and Raman microprobe techniques for the study of carbon materials. *J Mater Chem* 8(12):2875–2879